LUND UNIVERSITY

Shadow Fading Model for Vehicle-to-Vehicle Network Simulators

Abbas, Taimoor; Kåredal, Johan; Tufvesson, Fredrik

SOURCE:
1. Department of Electrical and Information Technology,
   Lund University,
   Lund, Sweden
2. Centre for Research on Embedded Systems,
   Halmstad University,
   Halmstad, Sweden

Shadow Fading Model for Vehicle-to-Vehicle

Network Simulations

1. Taimoor Abbas, Fredrik Tufvesson, Katrin Sjöberg, and Johan Kåredal

Taimoor Abbas
Department of Electrical and Information Technology
Lund University
Box 118, SE-22100
Lund, SWEDEN
Phone: + 46-46-2224902
Fax: + 46-46-129948
Email: taimoor.abbas@eit.lth.se

Shadow Fading Model for Vehicle-to-Vehicle Network Simulations

Taimoor Abbas, *Student Member, IEEE*, Fredrik Tufvesson, *Senior Member, IEEE*, Katrin Sjöberg, *Student Member, IEEE*, and Johan Karedal

Abstract—The Vehicle-to-Vehicle (V2V) propagation channel has significant implications on the design and performance of novel communication protocols for Vehicular Ad Hoc Networks (VANETs). Extensive research efforts have been made to develop V2V channel models to be implemented in advanced VANET system simulators for performance evaluation. The impact of shadowing caused by other vehicles has, however, largely been neglected in most of the models, as well as in the system simulations. In this paper we present a simple shadow fading model targeting system simulations based on real world measurements performed in urban and highway scenarios. The measurement data is separated for the situations like line-of-sight (LOS), the obstructed line-of-sight (OLOS) by vehicles, and non line-of-sight (NLOS) by buildings with the help of video information available during measurements. It is observed that the vehicles obstructing LOS induce an additional attenuation of about $10\,\mathrm{dB}$ in the received signal power. We use a Markov chain based state transition diagram to model transitions from LOS to obstructed LOS and present an example of state transition intensities for a real traffic mobility model. We also provide a simple recipe, how to incorporate our shadow fading model in VANET network simulators.

I. INTRODUCTION

Vehicle-to-Vehicle (V2V) communication allows vehicles to communicate directly and detect the positions of other vehicles with minimal latency. The primary objective is to improve active on-road safety and situation awareness, i.e., collision avoidance, traffic re-routing, navigation, etc. The propagation channel in V2V networks is significantly different from that in cellular networks because V2V networks are based on peer-to-peer communication where the communicating nodes are highly dynamic. Both the transmit (TX) and receive (RX) antennas are at the same height and close to ground level. Moreover, even if the propagation environment stays the same, the traffic density changes the channel parameters significantly. Thus, to develop an efficient and reliable system a deep understanding of V2V channel characteristics is required [1].

A number of V2V measurement campaigns have been performed to study the statistical properties of V2V propagation channels [2]–[6]. Signal propagation over the wireless channel is often divided by three statistically independent phenomena named deterministic path loss, small scale fading, and large-scale or shadow fading [7]. Path loss is the expected (mean) loss at a certain distance compared to the received power at a reference distance. The signal from TX can reach RX via several propagation paths and these multi-path components (MPC) can have different amplitudes and phase. A change in the signal amplitude due to constructive or destructive interference of the different MPCs is called small-scale fading. Finally, obstacles in the propagation paths of one or more MPCs cause great attenuation and the effect is called shadowing. Shadowing give rise to large-scale fading and it occurs not only for the line-of-sight (LOS) component but also for any other major MPC. Understanding of all these phenomena is equally important to characterize V2V propagation channel.

In real scenarios there can be light to heavy traffic, involving vehicles with variable speeds and heights, and there are sometimes buildings around the roadside. Hence, it might be the case that the LOS is obstructed by another vehicle or a house. The received power depends very much on the propagation environment, and the availability of LOS. Moreover, in [8] it is reported that, in the absence of LOS, most of the power is received by single bounce reflections from physical objects. Therefore for a realistic simulation and performance evaluation it is important that the channel parameters are separately characterized for LOS and NLOS conditions.

A number of different V2V measurements campaigns with their extracted channel parameters are comprehended in [9]. For most of the investigations mentioned above it is assumed that the LOS is available for the majority of recorded snapshots. Thus the samples from both the LOS and NLOS cases are lumped together for the modeling purpose due to dominance of LOS, which is somewhat unrealistic, especially for larger distances. The LOS path being blocked by buildings (NLOS) greatly impacts the reception quality in situations when vehicles are approaching the street intersection or road crossings. The buildings at the corners influence the received signal not only by blocking the LOS but also act as scattering point which helps to capture more power in the absence of LOS. A few measurement results for a NLOS environment are available [10]–[14] in which the path loss model is presented for different type of street crossings.

In addition to NLOS situation, the impact of neighboring vehicles can not be ignored. In [5] it is reported that the received signal strength gets worse on the same patch of an open road in heavy traffic hours as compared to no traffic hours. These observed differences can only be related to other vehicles obstructing LOS since the system parameters remained same

Fig. 1. Snapshot taken from the RX car, when the LOS was obstructed by a truck on a highway.

Fig. 2. Snapshot taken from the RX car, when the LOS became available on a highway.

during the measurement campaign. Similarly, Zhang *et. al.* in [15] presents an abstract error model in which the LOS and NLOS cases are separated using the thresholding distance. It is stated that the signals will experience more serious fading in crowded traffic scenario when the distance is larger than the thresholding distance. In [16] and [17] it is shown that the vehicles as obstacle have a significant impact on LOS obstruction in both the dense and sparse vehicular networks, therefore, shadow fading effects due to other vehicles are very important to be included in channel models. To date, in majority of the findings for V2V communications except [16] and [17], the shadowing impact of vehicles has largely been neglected when modeling the path loss. It is important to model vehicles as obstacles, ignoring this can lead to an unrealistic assumptions about the performance of the physical layer, which in turn can effect the behavior of higher layers of V2V systems. The channel properties for all three cases; LOS, the shadowing caused by other vehicles (OLOS), and, the LOS path being blocked by buildings (NLOS), are distinct and their individual analysis is required. No path loss model is available today dealing all three cases together in a comprehensive way.

The main contribution of this paper is a simple shadow fading model based on real world measurements in high-way and urban environments. The model targets Vehicular Ad Hoc Network (VANET) system simulations therefore we also provide simple recipe to distinguish LOS, OLOS and NLOS conditions in the simulator. We model state transitions from LOS to OLOS and NLOS by a Markov chain based state transition diagram and provide sample state transition intensities for a real traffic mobility model based on our measurements. We model temporal correlation of shadow fading as simple auto-regressive process. Finally, simulation results are presented where we compare the results obtained from our shadow fading model against the commonly used Nakagami-m pathloss model.

The rest of paper is organized as follows. Section II briefly reviews the measurement campaign for vehicle-to-vehicle communications and explains method to separate LOS, OLOS and NLOS data samples which serves as first step to model the effects of shadow fading. Section III covers methods for data analysis, as it includes derivation of path

loss and modeling of LOS and OLOS data as log-normal distribution. The channel model is provided in section IV. First the extension in traffic mobility models is suggested to include the effect of large-scale fading and then path loss model is presented and parameterized based on the measurements. VANET simulation results are discussed in Section V. Finally, section VI concludes the paper.

II. METHODOLOGY

A. Measurement Setup

Channel measurement data was collected using the RUSK-LUND channel sounder, which performs multiple-input multiple-output (MIMO) measurements based on the switched array principle. The measurement bandwidth was $200\,$MHz centered around carrier frequency of $5.6\,$GHz and a total $N_f = 641$ frequency points. For the analysis the complex time-varying channel transfer function $H(f,t)$ was measured, for two different time durations short term (ST), $25\,$s, and long term (LT), $460\,$s. The short-term and long-term channel transfer functions were composed of total $N_t = 49152$ and $N_t = 4915$ time samples, sampled with a time spacing of $\Delta t = 0.51\,$ms and $\Delta t = 94.6\,$ms, respectively. The test signal length was set to $3.2\mu\,$s.

Two standard $1.47\,$m high station wagons, Volvo V70 cars, were used during the measurement campaign. Four wide band omni-directional antennas, mounted at four different positions on each TX and RX, were used. Here we include results only for a roof mounted antennas. The roof antennas were taped on a Styrofoam block that, in turn, was taped to the shark fin on the center of the roof, side wise, and $360\,$mm from the back edge of the roof. Videos were taken through the windscreen of each TX/RX car and GPS data was also logged during each measurement. Video recordings and GPS data together with the measurement data were used in the post processing to identify LOS/OLOS/NLOS conditions, important scatterers and to keep track of distance between the two cars. The videos and the measurements were synchronized during measurements.
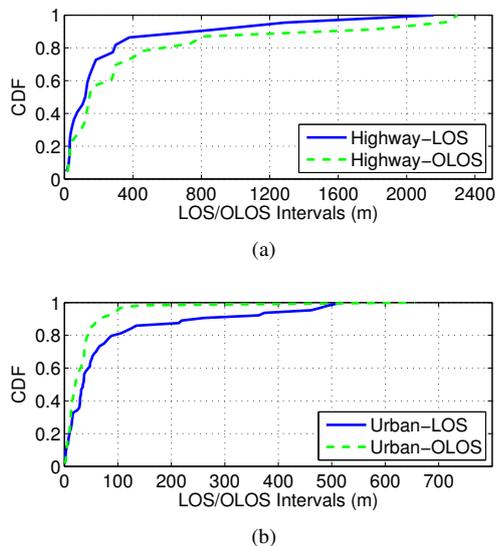
Fig. 3. Cumulative Distribution Function (CDF) of LOS and OLOS time intervals for all measurements; (a) highway scenario, (b) urban scenarios.

B. Measurement routes

Eight routes in two propagation environments were chosen with differences in their traffic densities, road-side environments, number of scatterers, pedestrians, and houses along the road side. All measurements were conducted in and in between the cities of Lund and Malmö, in the south of Sweden.

Highway; Measurements were performed, when both the TX and RX cars were moving in a convoy at a speed of $22 - 25$ m/s ($80 - 90$ km/h), on a 4 lane highway, 2 lanes in each direction. There were few to many vehicles moving in the opposite direction and also in the same direction as the TX and RX. Along the road side there were trees, vegetation, road signs, street lights and few buildings situated at random distances. The direction of travel was separated by a (≈ 0.5 m tall) concrete wall whereas the outer boundary of road was guarded by a metallic rail.

Urban; Measurements were performed, when both the TX and RX cars were moving in a convoy as well as in opposite directions, in densely populated areas in Lund and Malmö. TX and RX cars were moving with different speeds $0 - 14$ m/s ($0 - 50$ km/h), depending on the traffic situation. The $12 - 20$ m wide streets were either single or double lane including side walks on both sides, lined with $2 - 4$ storied buildings or trees on either side. Moreover, there were road signs, street lights, some trees, bicycles and many parked cars, mostly, on both sides and sometimes, only on a single side of the street. The streets were occupied with number of moving vehicles as well as few pedestrians walking on the sidewalks.

In total 3 short term (ST) and 2 long term (LT) measurements for highway, and, 7 short term (ST) and 4 long term (LT) measurements for urban-convoy were performed. During each measurement, often the LOS was obstructed by other cars, taller vans, trucks, buses, or, houses at the street corner. For the subsequent analysis we separate the LOS, OLOS and NLOS cases for all the measurements and perform the analysis based on extracted information.

C. LOS, OLOS and NLOS separation

To separate the LOS from OLOS and NLOS cases we make use of geometric information available from the videos, taken during the measurements. LOS condition is defined as when it is possible for one of the cameras to see the middle of the roof of the other vehicle. Otherwise we say that the LOS is blocked. The blocked LOS situation is further categorized in two groups; when one or more vehicles obstruct the LOS path, OLOS, and, when the buildings block the LOS path, NLOS. When blocked by buildings, and cars are not aligned with each other, NLOS is defined using a map as if it is not possible to make a straight line between the two vehicle positions without being obstructed by a building.

From electromagnetic wave propagation point of view, impact of an obstacle can be assessed qualitatively, by the concept of the Fresnel ellipsoids. It is required to have Fresnel zone free of obstacles in order to have LOS and only the visual sight does not promise the availability of LOS [7]. If the obstacle does not obstruct the visual sight but the Fresnel ellipsoid, partially or completely, it may have some impact on the strength of the received signal. The availability of LOS based on Fresnel ellipsoids depends very much on the information about height of obstacle, its distance from TX and RX, the direct distance between TX and RX as well as the wavelength λ. Since, the videos and the measurement data do not include detailed information about obstacles, such as, their height and their relative distance from TX and RX at each instant, it is very hard to take Fresnel zone into account while separating the LOS samples from OLOS and NLOS. With this limitation the visual sight seem to be the best solution for a straightforward separation process.

TABLE I
AVERAGE DISTANCE TRAVELED IN LOS AND OLOS CONDITIONS.

	Scenario	min	max	mean	median
LOS Intervals (m)	Highway	24.4	2157	299	125
	Urban	0.95	519	84.6	35.3
OLOS Intervals (m)	Highway	18.6	2298	467	150
	Urban	2.4	656	39.8	20.5

III. ANALYSIS

In our measurement campaign, we drove in total 8256 m in Urban and 17343 m in Highway environment. In the presence of LOS; we drove 5477 m in Urban and 6622 m in Highway environment, in OLOS by cars; we drove 2429 m in Urban and 10752 m in Highway environment, and, in NLOS by building; we drove 415 m in Urban and 0 m in Highway environment. During the whole measurement run the TX-RX link transited from LOS to OLOS/NLOS and back, a number of times, i.e., LOS-OLOS; 61 times in urban and 23 times in highway scenario, similarly, LOS-NLOS; 4 times in urban and 0 times in highway scenario. No transition took place from OLOS to NLOS. Each time the TX-RX pair is in one of the LOS, OLOS or NLOS state, it remains in that state for some time interval. The Cumulative Distribution Function (CDF) of these time intervals are shown in Fig. 3(a), and 3(b). The distance

traveled by RX corresponding to each LOS and OLOS time intervals is parameterized in Table I. The NLOS do not usually occur on highways, moreover, the data samples for NLOS data in our urban measurements are not enough therefore it is not shown as histogram.

A. Pathloss Derivation

The time varying power-delay-profile (PDP) is derived for each time sample in order to determine the path loss. The effect of small scale fading is eliminated by averaging the time varying PDP over N_{avg} number of time samples and let the averaged-PDP (APDP) be given by [18] as,

$$P_h(t_k, \tau) = \frac{1}{N_{avg}} \sum_{n=0}^{N_{avg}-1} |h(t_k + n\Delta t, \tau)|^2, \quad (1)$$

for $t_k = 0, N_{avg}\Delta t, ..., \lfloor N_t/N_{avg} - 1 \rfloor N_{avg}\Delta t$, where $h(t_k + n\Delta t, \tau)$ is the complex time varying channel impulse response derived by an inverse Fourier Transform of a Channel Transfer function $H(f, t)$ for single-input single-output (SISO) antenna configuration. The N_{avg} is calculated by $N_{avg} = \frac{s}{v\Delta t}$, where Δt is the time spacing between snap shots, s corresponds to the movement of TX and RX by 15 wavelengths and v is the velocity of TX and RX given in each scenario description.

The zeroth order moment of the noise thresholded, small-scale averaged APDPs gives the averaged channel gain for each link as,

$$G_h(t_k) = \frac{1}{N_\tau} \sum_\tau P_h(t_k, \tau), \quad (2)$$

where τ is the propagation delay. The cable attenuation and the effect of low-noise-amplifier (LNA) were removed from the measured gains. Hence, the channel gains presented in the paper are the gains experienced from the TX antenna connector to the RX antenna connector. Moreover, noise thresholding of each APDP is performed by allowing all signals with power below the noise floor, i.e., noise power plus a $3\,\text{dB}$ additional margin, to zero. The noise power is determined from the part of PDP, at larger delays, where no contribution from the transmitted signal is present.

The path loss $PL(d)$ is equal to the negative of the distance dependent channel gain $G_h(d)$, which is obtained by matching the time dependent channel gain $G_h(t_k)$ to its corresponding distance d between TX and RX at time instant t_k. We used GPS data, recorded during the measurements, to find the distance between TX and RX which corresponds to the propagation distance of first arriving path for each time sample in the presence of line-of-sight. Since the time resolution of the GPS data was limited (one GPS position/second). Thus, to make GPS data sampling rate equal to the time snapshots, we applied interpolation of the GPS data with *cubic splines* method. The distance obtained from the GPS data was validated, later, by tracking the first arrived MPC, in the presence of LOS, with a high resolution tracking algorithm [19].
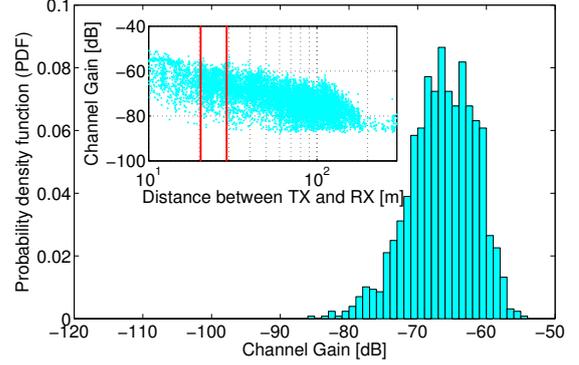

Fig. 4. Inset plot shows overall channel gain for urban measurement data as a function of direct distance between TX and RX. Large plot is the histogram of channel gains taken from log spaced distance bin, marked by vertical lines in the inset plot, $20.4 - 29.1\,\text{m}$. The LOS and OLOS data is taken together in this figure.
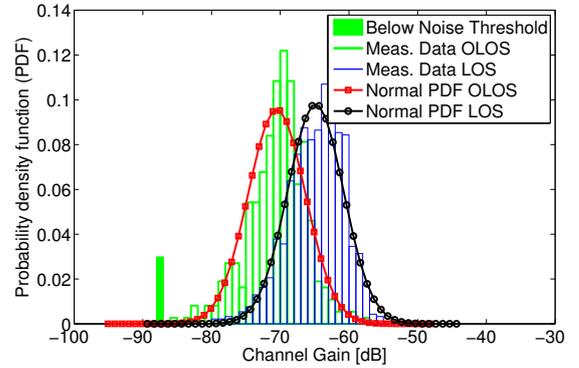
Fig. 5. Histogram of the same channel gains as in Fig. 4, when separated as LOS and NLOS. The data is taken from log spaced distance bin $20.4 - 29.1\,\text{m}$ from the urban measurement data; pdf fitting the normal distribution.
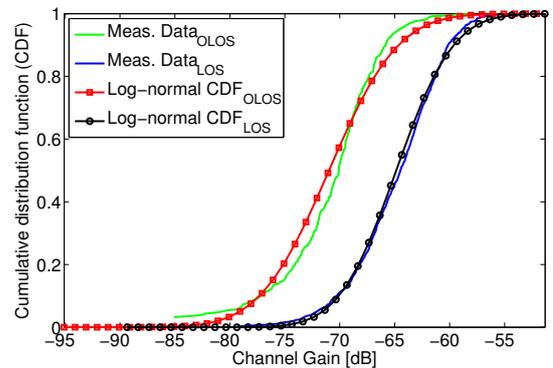

Fig. 6. The separated LOS and OLOS data taken from log spaced distance bin $20.4 - 29.1\,\text{m}$ from the Urban measurement data; cdf fitting the log-normal distribution with 95% confidence interval.

B. Large-scale fading

As explained earlier the effect of small scale fading is removed by averaging the received signal power over a distance of a few wavelengths. The averaged envelope is a random variable due to the large-scale variations caused by the shadowing from large objects such as building, and vehicles. The most widely accepted approach is to model the large-scale variations with a log-normal distribution function [7], [20]. For the analysis we divide the distance dependent channel gain, $G_h(d)$, data with respect to log-spaced distance bins and independently study the distribution of data associated to each bin. When we tried to model our measurement data for each distance bin, before separating the LOS, OLOS and NLOS data samples, it was observed that a log-normal distribution does not provide a good match with the observed data (see, e.g., Fig. 4). Moreover, apparently an additional attenuation was observed which makes the spread in the channel gain large and the spread was different for different distance bins. As a first guess, the attenuation could possibly be associated to the obstruction of LOS. Therefore, to find the data distribution the LOS, the OLOS, and the NLOS data was analyzed separately. Interestingly it is observed that the large-scale variations for both the LOS and the OLOS data sets can be modeled to be log-normally distributed (see, e.g., Fig. 5, 6) with an offset of almost $10\,\mathrm{dB}$ in their mean. This observation go well in line with the independent observations presented in [17]. The channel gain in the OLOS condition, at instants, falls below the noise floor of the channel sounder and power levels of samples below the noise threshold can not be detected correctly. It is observed that the OLOS data in each bin for shorter distances, with no missing samples, fits well to the log-normal distribution and we assume that the data continues to follow log-normal distribution for larger distance bins where the observed data is incomplete. Moreover, the exact count of missing samples is also available which can be used to estimate the overall data distribution. To get the higher order statistics of normally distributed LOS and OLOS data we compute the maximum likelihood estimates (MLE) of scale and position parameters from incomplete data by [21] where Dempster *et. al.* presents a broadly applicable algorithm which iteratively computes MLE from incomplete data via expectation maximization (EM).

IV. CHANNEL MODEL

In this section a very simple large-scale fading model for VANET simulations is provided. This model is targeting network simulations, where there is a need for a realistic but simple model taking shadowing effects into account. Further, a Markov model is used as a basis for the mobility model. State transition intensities for vehicles are extracted from measurements, which can be used for modeling the time duration in LOS, OLOS, and NLOS state, respectively. The Markov model approach has the advantage that it introduces correlated path loss levels (through the states), a property that we think is important for more realistic network simulations. However, for this type of analysis the measurement data set is constrained therefore, these intensities can only be treated

as an example. The existing traffic mobility models already provide instantaneous position of vehicles and by simple geometric manipulation it is easy to identify whether the TX and RX vehicles are in LOS, OLOS or NLOS state, which makes this model easy to implement in many VANET simulators.

A. Extension in the Traffic Mobility Models

Today's traffic mobility models implemented in VANET simulators are very advanced, e.g., SUMO (Simulation of Urban Motility) [22] is one example of such an open source mobility model. These advanced models are capable to take into account the vehicle position, exact speed, inter vehicle spacing, acceleration, overtaking attitude, lane-change behaviors, etc. However, the possibility of treating the vehicles as obstacles and modeling the intensities by which they obstruct the LOS for other vehicles are still missing in the simulators. Therefore, a simple extension for including shadowing effects in network simulators is provided herein. Since the vehicular mobility models implemented in the simulators give instantaneous information about each vehicle, shadow fading can be implemented by simple geometric manipulation as follows.

- Model each vehicle or building as a rectangle in the simulator.
- Draw a straight line starting from the antenna position of each TX vehicle to the antenna position of each RX vehicle.
- If the line does not touch any other rectangle, TX/RX has LOS.
- If the line passes through another rectangle, LOS is obstructed by a vehicle or by a building, the two cases can easily be distinguished by using the geographical information available in simulator.
- Once the propagation condition is identified, the simulator can simply use the relevant model to calculate the power loss.

TABLE II
STATE TRANSITION INTENSITIES IN OUR MEASUREMENTS.

Trans. Intensities(m^{-1})	P	p	Q	q	R	r
Highway	0.0035	0.0020	0	0	0	0
Urban	0.0111	0.0245	0.00073	0.0095	-	-

To further simplify the implementation, the vehicles can also be modeled as circles with antenna position as a center and the width of a standard car as a diameter of the circle. If a mobility model is not available, state transition intensities can be used directly. The measurement data contains geometric information about when the LOS, OLOS, and NLOS conditions occur and their respective durations. Therefore, state transition intensities are easily calculated. However, these intensities are specific to the environment, the driver attitude and the traffic density during the measurement campaign. For the large-scale fading model we use a Markov chain with three states and its working principle is the same as the Gilbert-Elliot model [23]. The state transition diagram for the traffic mobility model is shown in Fig. 7 and the state transition intensities are
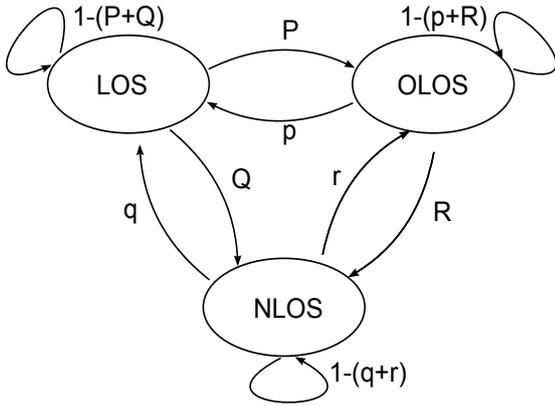
Fig. 7. State transition diagram for the Traffic Mobility Model (TMM).

provided in Table II. A similar approach was used in [24] where a lightweight model to evaluate the impact of vehicle's mobility and their incorporation was modeled as a Markov chain process.

Transitions between the different states in Fig. 7 take no time. The state transition intensities, P, p, Q, q, R, r are calculated from the measurements, simply, by dividing the number of transitions from one state to another with the total distance traveled in initial state. For example, the intensity $P = N_{LOS \to OLOS}/S_{LOS} = 0.0111 m^{-1}$, when $S_{LOS} = 5412$ m is the distance traveled in LOS state and $N_{LOS \to OLOS} = 61$ is the number of transitions from LOS to OLOS. Other intensities are calculated in a similar way. Again, if geometrical data is available from a mobility model, the states can be derived directly from there, and no transition intensities are needed for the simulations.

TABLE III
PARAMETERS FOR THE DUAL-SLOPE PATH LOSS MODEL

	Scenario	n_1	n_2	PL_0	σ	d_c
LOS	Highway	-1.66	-2.88	-58.7	3.95	23.25
	Urban	-1.81	-2.85	-56.5	4.15	4.25
OLOS	Highway	-	-3.18	-68.7	6.12	32.5
	Urban	-1.93	-2.74	-66.5	6.67	4.5

B. Pathloss Model

The measurement data is split into three data sets; LOS, OLOS and NLOS. The parameters of the path loss model are extracted only for the LOS and the OLOS data sets, whereas, not enough data is available to model the path loss for the third, NLOS, data set.

The measured channel gain for LOS and OLOS data for the highway and the urban scenario is shown as a function of distance in Fig. 8 and 9, respectively. A simple log-distance power law [7] is often used to model the path loss to predict the reliable communication range between the transmitter and the receiver. The generic form of this log-distance power law path loss model is given by,

$$PL(d) = PL_0 + 10n \log_{10}\left(\frac{d}{d_0}\right) + X_\sigma, \qquad (3)$$

where d is the direct distance between TX and RX, n is the path loss exponent estimated by linear regression and X_σ is zero-mean normal distributed random variable with standard deviation σ and possibly with some time correlation. PL_0 is the free-space path loss plus the accumulative antenna gain ($PL_0 = PL_f + G_a$) at a reference distance d_0 in dB. The antenna gain was not measured when mounted on the roof of the car, therefore a subtraction of the antenna gain from the measured data is not possible.

In practice it is observed that the dual-slope model, as stated in [25], can represent measurement data more accurately. We thus characterize dual-slope model as piecewise-linear model with the assumption that the power decays with path loss exponent n_1 and standard deviation σ_1 until the a breakpoint distance (d_b) and from there it decays with path loss exponent n_2 and standard deviation σ_2. The dual-slope model be given by,

$$PL(d) = \begin{cases} PL_0 + 10n_1 \log_{10}\left(\frac{d}{d_0}\right) + X_\sigma, & \text{if } d_0 \le d \le d_b \\ PL_0 + 10n_1 \log_{10}\left(\frac{d_b}{d_0}\right) + & \text{if } d > d_b \\ 10n_2 \log_{10}\left(\frac{d}{d_b}\right) + X_\sigma, & \end{cases}$$

$$(4)$$

The distance between TX and RX is extracted from the GPS data which can be unreliable when TX-RX are very close to each other. Moreover, there are only a few samples available for $d < 10$, thus the validity range of the model is set to $d > 10$ and let $d_0 = 10$. The typical flat earth model consider d_b as the distance at which the first Fresnel zone touches the ground or the first ground reflection has traveled $d_b + \lambda/4$ to reach RX. For the measurement setup the height of the TX/RX antennas was $h_{TX} = h_{RX} = 1.47$ m, so, d_b can be calculated as, $d_b = \frac{4h_{TX}h_{RX} - \lambda^2/4}{\lambda} = 161$ m for $\lambda = 0.0536$ m at 5.6 GHz carrier frequency. A d_b of 104 m was selected to match the values with the path loss model presented in [25], it also implies a somewhat better fit to the measurement data.

The path loss exponents before and after d_b in (4) are adjusted to fit the median values of the LOS and OLOS data sets in least square sense and are shown in Figs. 8 and 9. The extracted parameters are listed in Table III. For the highway measurements OLOS occurred only when the TX/RX vehicles were widely separated, i.e., when $d > 80$ m, which means that there are too few samples to model the path loss exponent in OLOS for shorter distances. Whereas in practice, this is not always the case, the OLOS can occur at shorter distances if there is traffic congestion on a highway with multiple lanes. Thus, the path loss exponent for OLOS for shorter distances is the same as in LOS.

It is interesting to notice that the slopes are not that different but there is an offset in the channel gain for LOS and OLOS data sets which is of the order of $9-10$ dB and is very similar to the results previously been reported. In [16] an additional attenuation of 9.6 dB is attributed to the impact of vehicle as an obstacle. Meireles *et. al.* in [17] states OLOS can cause $10-20$ dB of attenuation depending upon traffic conditions.

It is highly important to model the path loss in the NLOS situation because power level drops quickly when the LOS
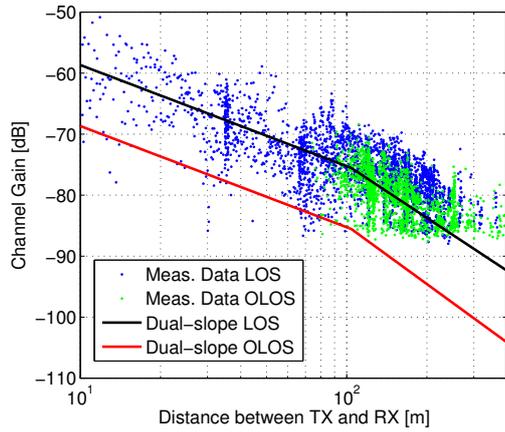
Fig. 8. Measured channel gain for the highway environment and the least square best fit to the deterministic part of (3).
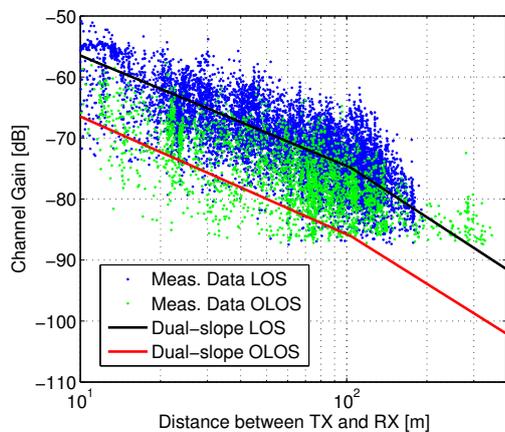

Fig. 9. Measured channel gain for the urban environment and the least square best fit to the deterministic part of (3).

is blocked by buildings. As mentioned above, the available measured data in NLOS is not sufficient to model the path loss therefore it is derived from available models specifically targeting similar scenarios, such as, [11], [12], [26] and COST 231-Welfish-Ikegami model (Appendix 7.B in [7]). Among these, Mangel *et. al.* in [12] presents a realistic and a well validated NLOS path loss model which is of low complexity, thus, enabling large-scale packet level simulations in intersection scenarios. The basis for the path loss equation in [12] is a cellular model proposed in [26], which is slightly modified to correspond well to V2V measurements. For completeness the Mangel's model [12] is used for the NLOS situation and it is given as follows,

$$PL(d_r, d_t, w_r, x_t, i_s) = 3.75 + i_s 2.94$$

$$+ \begin{cases} 10 \log_{10}\left(\left(\frac{d_t^{0.957}}{(x_t w_r)^{0.81}} \frac{4\pi d_r}{\lambda} \right)^{n_{NLOS}} \right), & \text{if } d_0 \le d_r \le d_b \\ 10 \log_{10}\left(\left(\frac{d_t^{0.957}}{(x_t w_r)^{0.81}} \frac{4\pi d_r^2}{\lambda d_b} \right)^{n_{NLOS}} \right), & \text{if } d_r > d_b \end{cases}$$

$$(5)$$

where d_r/d_t are distance of TX/RX to intersection center, w_r is width of RX street, x_t is distance of TX to the wall,

and i_s specifies suburban and urban with $i_s = 1$ and $i_s = 0$, respectively. In the network simulator the road topology and TX/RX positions are known, so, these parameters can be obtained easily. The path loss exponent in NLOS is provided in the model as $n_{NLOS} = 2.69$ and normal distributed fading with $\sigma = 4.1\,\text{dB}$.

For larger distance ($d_r > d_b$) the model introduces increased loss due to diffraction, around the street corners, being dominant. The model is developed for TX/RX in adjacent streets. If the TX/RX are not in adjacent streets but in parallel streets with building blocking the LOS then this NLOS model is not sufficient. The direct communication in such setting might not be possible or not required but these cars can introduce interference for each other due to diffraction over roof tops. This propagation over the roof top can be well approximated by diffraction by multiple screens as it is done in the COST 231 model. However, in [27] simulation results are shown which state that the path loss in non-adjacent street is always very high, $> 120\,\text{dB}$. The value is similar to the one obtained with theoretical calculations for diffraction by multiple screens. As the losses for the vehicles in parallel streets are high, interference from such vehicles can simply be ignored.

C. Spatial Correlation of Shadow Fading

V2V networks use cooperative awareness messages (CAM) for road safety, traffic efficiency and other applications. Applications in each of these category have different requirements w.r.t. latency and geografical coverage. CAM use a broadcast mode to state vehicles existence to the neighboring nodes. When a link goes into a shadow region, it remains there for some time. If the vehicle is in a shadow region its existence may not be noticed for some time. Hence, it is important to study the spatial correlation of shadow fading as part of the analysis.

The large-scale variation of shadow fading can be well described as a Gaussian random variable (discussed in section III). By subtracting the distance dependent mean from the overall channel gain the shadow fading can be assumed a stationary process. Then the spatial auto-correlation of the shadow fading can be written as,

$$r_x(\Delta d) = E\{X_\sigma X_\sigma(d + \Delta d)\}. \tag{6}$$

The auto-correlation of the Gaussian process can then be modeled by a well-known analytical model proposed by Gudmundson [28], which is a simple negative exponential function,

$$r_x(\Delta d) = e^{-|\Delta d|/d_c}, \tag{7}$$

where Δd is as equally spaced distance vector and d_c is a decorrelation distance which is scenario-dependent real valued constant. In Gudmundson model, d_c is defined as the value of Δd at which the value of the auto-correlation function $r_x(\Delta d)$ is equal to $1/e$. The value of the decorrelation distance d_c is determined from both the LOS and OLOS measured auto-correlation functions and are given in Table III, for both
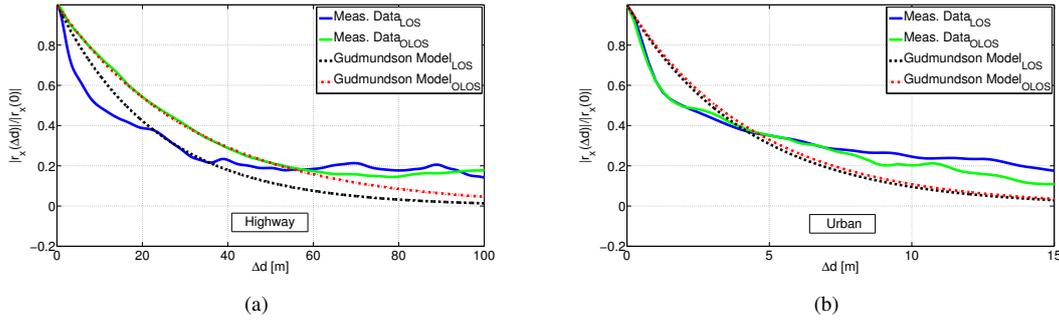
Fig. 10. Measured auto-correlation function and model according to (7) for LOS and OLOS data; (a) highway scenario, (b) urban scenarios.

the highway and urban scenarios, respectively. The estimated correlation distance is thus used to model the measured auto-correlation functions using (7), and is shown in Fig. 10(a) and 10(b).

Looking at decorrelation distances d_c, the implementation of shadow fading in the simulator can be simplified by treating it as a block shadow fading, where d_c can be assumed as a block length in which the signal power will remain, more or less, constant.

V. NETWORK SIMULATIONS

Finally, we include V2V network simulations to support our claim that the LOS obstruction by vehicles degrades the performance of vehicular networks. The simulation scenario is a 10 km long highway with 12 lanes (six lanes in each direction). The vehicles appear with a Poisson distribution with two different inter-arrival rates, depending on investigated vehicle density. Every vehicle broadcasts 400 byte long position messages (i.e. CAMs) 10 times/sec (10 Hz) using a transfer rate of 6 Mbps and an output power of 20 dBm (100 mW). The channel access procedure is self-organizing time division multiple access (STDMA) [29] that has been proposed as medium access control (MAC) method for VANETs [30] [31]. The vehicle speeds are independently Gaussian distributed with a standard deviation of 1 m/s, with different mean values (23 m/s, 30 m/s, 37 m/s) depending on lane. The vehicles maintain the same speed as long as they are on the highway. The shadowing based channel model presented herein has been compared against a traditional Nakagami-m model [25] in the network simulations, where the latter is not capable of distinguishing between LOS and OLOS. The Nakagami-m model is also based on an outdoor channel sounding measurement campaign, performed at 5.9 GHz. The small-scale fading and the shadowing are both represented by the Nakagami-m model [25]. The fading intensities, represented by the m parameter of the Nakagami distribution, are different depending on the distance between TX and RX, and the m values are taken from data set 2 in [25]. The averaged received power for the Nakagami model is computed using the following formula:

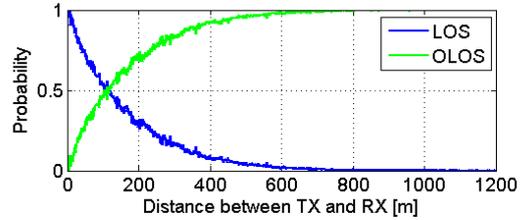$$P_{RX}(d) = P_{TX} - PL(d) - P_{IL} + G_a \qquad (8)$$

Fig. 11. The probabilities of being in LOS and OLOS, respectively, depending on distance between TX and RX.

where $PL(d)$ is calculated as equation 4 with theoretical path loss exponents $n_1 = 1.9$ and $n_2 = 3.8$. In the model the antenna gain is included in the channel gain, therefore the total difference in power PL_0 at d_0 is 9.1 dB between the Lund-LOS and Nakagami model [25]. The difference is assumed as antenna gain, with 4.5 dB antenna gain for each TX/RX. Compensating for this antenna gain, the reference levels are the same in LOS for the proposed model and for the Nakagami model. In addition to that the compensation for implementation losses must be done, i.e., cable losses. If a 2 m long cable is used on each side (TX and RX), assuming a cable loss of 1.7 dB/m, then a total loss of 6.8 dB is received. If this implementation loss P_{IL} is removed the PL_0 will be close to 65.5 dB, which resembles the free space path loss.

The averaged received power for the LOS part, the OLOS part and the Nakagami m model, is depicted in Fig. 12. At shorter distances there is little chance that another vehicle is between any two communicating vehicles but as the distance increases the chances of being under OLOS either by vehicle, object, or due to the curvature of the earth, increases. The probabilities of being in LOS and being in OLOS have been calculated from the network simulator for the highway scenario and are depicted in Fig. 11. To receive the averaged power similar to the Nakagami model these probabilities can be multiplied with the averaged received power for LOS and OLOS at different distances using the following equation:

$$P_{RX}(d) = Prob(LOS|d)P_{RX-LOS}(d)$$
$$+ Prob(OLOS|d)P_{RX-OLOS}(d) \qquad (9)$$

By using Eq. 9 the averaged received power for the LOS and OLOS conditions coincides with the Nakagami averaged
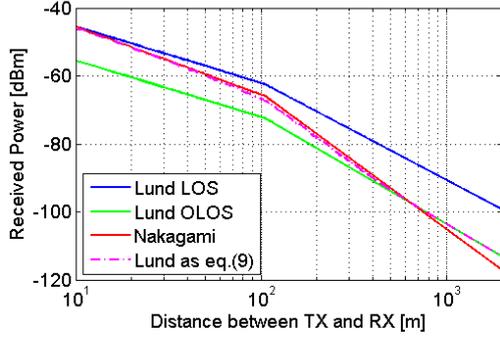
Fig. 12. The averaged received power for the LOS/OLOS model and the Nakagami model, respectively.
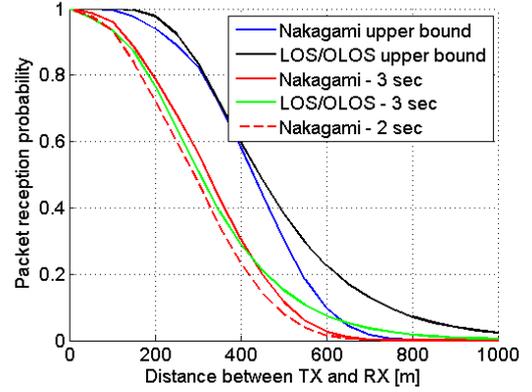

Fig. 13. Packet reception probability for the LOS/OLOS model and the Nakagami model compared against the upper bound for each channel model.
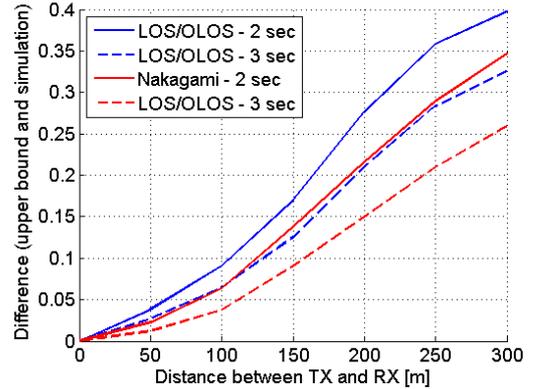

Fig. 14. The difference between the upper bound and the simulation for the two different channel models is depicted.

received power, see Fig. 12, which is very interesting to notice.

In Fig. 13 the packet reception probability averaged over all RXs within a certain distance from a TX is depicted for the two different channel models. The two upper bound curves show the packet reception probability for a system with no interference, i.e., no other transmission is ongoing at any place in the network. This is the best performance that can be achieved with the two different channel models and therefore, this is called an upper bound. Two different inter-arrival rates of vehicles have been used; two seconds and three seconds. Two seconds yield a vehicle density of 12-13 vehicles/km/lane and three seconds yield a vehicle density of 9-10 vehicles/km/lane. Between 300-400 meters the upper bound curves for both channel models more or less coincide. The upper bound curve for the LOS/OLOS model is slightly better for longer distances due to the averaged received power for this model is higher for longer distances, see Figure 13(b).

Both channel models experience similar performance degradation when increasing the vehicle density. In Fig. 14 the difference between the upper bound and the simulations results for each channel model, respectively, is depicted. The solid lines are showing the higher vehicle density case and there is performance degradation of up to 8% when considering LOS/OLOS receptions compared to the Nakagami model, which is a considerable loss.

Further, simulations will be conducted using the MAC method carrier sense multiple access (CSMA), which has been selected as the channel access procedure for the first generation of vehicle-to-vehicle communications systems. In STDMA, a node is always granted access to the medium regardless of the number of nodes within radio range and when the system is overloaded nodes transmit at the same time as someone else in the system situated furthest away from itself. Therefore, STDMA needs position information which is present in the position messages transmitted (i.e., CAMs). The scheduling of transmission in space implies that STDMA can maintain a high packet reception probability for the nodes situated closest to the transmitter.

VI. SUMMARY AND CONCLUSIONS

In this paper a simple shadow fading model based on measurements performed in urban and highway scenarios is presented, where a separation between LOS, obstructed LOS by vehicle (OLOS) and obstructed LOS by building (NLOS), is performed. In the past, despite extensive research efforts to develop more realistic channel models for vehicle-to-vehicle (V2V) communication, the impact of vehicles obstructing LOS has largely been ignored. We have observed that the LOS obstruction by vehicles (OLOS) induce an additional loss, of about 10 dB, in the received power. Network simulations have been conducted showing the difference between a traditional Nakagami based channel model (often used in VANET simulations) and the LOS/OLOS model presented herein. There is considerable performance degradation for the LOS/OLOS model compared to the Nakagami model. We thus conclude that the obstruction of LOS cannot be ignored when evaluating the performance of V2V communications and there is a need for a LOS/OLOS model in VANET simulators. Further, if it does not exist a mobility model in the VANET simulator the state transition intensities principle presented herein can be used for modeling the LOS and OLOS states. Probabilities for state transition intensities have been provided based on the measurements. . The LOS/OLOS model is easy to implement in VANET simulators due to the usage of a dual-piece wise path loss model and the shadowing effect is modeled using a zero-mean Gaussian distribution.

REFERENCES

[1] J. Gozalvez, M. Sepulcre, and R. Bauza, "Impact of the radio channel modelling on the performance of VANET communication protocols," *Telecommunication Systems*, pp. 1–19, Dec. 2010.

[2] G. Acosta-Marum and M. Ingram, "Six time- and frequency- selective empirical channel models for vehicular wireless LANs," *IEEE Veh. Technol. Mag.*, vol. 2, no. 4, pp. 4–11, 2007.

[3] I. Sen and D. W. Matolak, "Vehicle-vehicle channel models for the 5 GHz band," *IEEE Trans. Intell. Transp. Syst.*, vol. 9, no. 2, pp. 235–245, Jun. 2008.

[4] A. Paier, J. Karedal, N. Czink, C. Dumard, T. Zemen, F. Tufvesson, A. F. Molisch, and C. F. Mecklenbräuker, "Characterization of vehicle-to-vehicle radio channels from measurements at 5.2 GHz," *Wireless Personal Commun.*, vol. 50, pp. 19–29, 2009.

[5] J. Otto, F. Bustamante, and R. Berry, "Down the block and around the corner the impact of radio propagation on inter-vehicle wireless communication," in *Distributed Computing Systems, 2009. ICDCS '09. 29th IEEE International Conference on*, june 2009, pp. 605 –614.

[6] O. Renaudin, V. M. Kolmonen, P. Vainikainen, and C. Oestges, "Non-stationary narrowband MIMO inter-vehicle channel characterization in the 5 GHz band," *IEEE Trans. Veh. Technol.*, vol. 59, no. 4, pp. 2007–2015, May 2010.

[7] A. Molisch, *Wireless Communications*. John Wiley & Sons, 2010.

[8] T. Abbas, J. Karedal, F. Tufvesson, A. Paier, L. Bernado, and A. Molisch, "Directional analysis of vehicle-to-vehicle propagation channels," in *Vehicular Technology Conference (VTC Spring), 2011 IEEE 73rd*, may 2011, pp. 1 –5.

[9] A. F. Molisch, F. Tufvesson, J. Karedal, and C. F. Mecklenbräuker, "A survey on vehicle-to-vehicle propagation channels," in *IEEE Wireless Commun. Mag.*, vol. 16, no. 6, 2009, pp. 12–22.

[10] T. Mangel, M. Michl, O. Klemp, and H. Hartenstein, "Real-world measurements of non-line-of-sight reception quality for 5.9 GHz IEEE 802.11p at intersections," *Communication Technologies for Vehicles, Springer Berlin Heidelberg*, vol. 6596, pp. 189–202, 2011.

[11] E. Giordano, R. Frank, G. Pau, and M. Gerla, "Corner: a realistic urban propagation model for vanet," in *Wireless On-demand Network Systems and Services (WONS), 2010 Seventh International Conference on*, feb. 2010, pp. 57 –60.

[12] T. Mangel, O. Klemp, and H. Hartenstein, "5.9 ghz inter-vehicle communication at intersections: a validated non-line-of-sight path-loss and fading model," *EURASIP Journal on Wireless Communications and Networking*, vol. 2011, no. 1, p. 182, 2011.

[13] P. Paschalidis, A. Kortke, K. Mahler, M. Wisotzki, W. Keusgen, and M. Peter, "Pathloss and Multipath Power Decay of the Wideband Car-to-Car Channel at 5.7 GHz," in *IEEE 73th Vehicular Technology Conference (VTC2011-Spring)*, Budapest, Hungry, May 2011.

[14] J. Turkka and M. Renfors, "Path loss measurements for a non-line-of-sight mobile-to-mobile environment," in *ITS Telecommunications, 2008. ITST 2008. 8th International Conference on*, oct. 2008, pp. 274 –278.

[15] Y. Zang, L. Stibor, G. Orfanos, S. Guo, and H.-J. Reumerman, "An error model for inter-vehicle communications in highway scenarios at 5.9 GHz," in *Proceedings of the 2nd ACM international workshop on Performance evaluation of wireless ad hoc, sensor, and ubiquitous networks*, ser. PE-WASUN '05. New York, NY, USA: ACM, 2005, pp. 49–56.

[16] M. Boban, T. Vinhoza, M. Ferreira, J. Barros, and O. Tonguz, "Impact of vehicles as obstacles in vehicular ad hoc networks," *Selected Areas in Communications, IEEE Journal on*, vol. 29, no. 1, pp. 15 –28, january 2011.

[17] R. Meireles, M. Boban, P. Steenkiste, O. Tonguz, and J. Barros, "Experimental study on the impact of vehicular obstructions in vanets," in *Vehicular Networking Conference (VNC), 2010 IEEE*, dec. 2010, pp. 338 –345.

[18] J. Kredal, N. Czink, A. Paier, F. Tufvesson, and A. Molisch, "Path loss modeling for vehicle-to-vehicle communications," *IEEE Transactions on Vehicular Technology*, vol. 60, no. 1, pp. 323–328, 2011.

[19] J. Karedal, F. Tufvesson, N. Czink, A. Paier, C. Dumard, T. Zemen, C. Mecklenbräuker, and A. F. Molisch, "A geometry-based stochastic MIMO model for vehicle-to-vehicle communications," *IEEE Transactions on Wireless Communications*, vol. 8, no. 7, pp. 3646–3657, 2009.

[20] G. Stüber, *Principles of Mobile Communication*. Dordrecht: Kluwer Academic Publishers, 1996.

[21] A. P. Dempster, N. M. Laird, and D. B. Rubin, "Maximum likelihood from incomplete data via the em algorithm," *JOURNAL OF THE ROYAL STATISTICAL SOCIETY, SERIES B*, vol. 39, no. 1, pp. 1–38, 1977.

[22] M. Behrisch, L. Bieker, J. Erdmann, and D. Krajzewicz, "SUMO - simulation of urban mobility: An overview," in *SIMUL 2011, The Third International Conference on Advances in System Simulation*, Barcelona, Spain, October 2011, pp. 63–68.

[23] E. N. Gilbert, "Capacity of a burst-noise channel," *Bell System Technical Journal*, vol. 39, pp. 1253–1265, 1960.

[24] D. Dhoutaut, A. Régis, and F. Spies, "Impact of radio propagation models in vehicular ad hoc networks simulations," in *Proceedings of the 3rd international workshop on Vehicular ad hoc networks*, ser. VANET '06. New York, NY, USA: ACM, 2006, pp. 40–49. [Online]. Available: http://doi.acm.org/10.1145/1161064.1161072

[25] L. Cheng, B. Henty, D. Stancil, F. Bai, and P. Mudalige, "Mobile vehicle-to-vehicle narrow-band channel measurement and characterization of the 5.9 ghz dedicated short range communication (dsrc) frequency band," *Selected Areas in Communications, IEEE Journal on*, vol. 25, no. 8, pp. 1501 –1516, oct. 2007.

[26] H. El-Sallabi, "Fast path loss prediction by using virtual source technique for urban microcells," in *Vehicular Technology Conference Proceedings, 2000. VTC 2000-Spring Tokyo. 2000 IEEE 51st*, vol. 3, 2000, pp. 2183 –2187 vol.3.

[27] T. Gaugel, L. Reichardt, J. Mittag, T. Zwick, and H. Hartenstein, "Accurate simulation of wireless vehicular networks based on ray tracing and physical layer simulation," in *High Performance Computing in Science and Engineering '11*, W. E. Nagel, D. B. Krner, and M. M. Resch, Eds. Springer Berlin Heidelberg, 2012, pp. 619–630.

[28] M. Gudmundson, "Correlation model for shadow fading in mobile radio systems," *Electronics Letters*, vol. 27, no. 23, pp. 2145 –2146, nov. 1991.

[29] Recommendations ITU-R M.1371-4, "Technical characteristics for an automatic identification system using time-division multiple access in the VHF maritime mobile band," 2010.

[30] K. Bilstrup, E. Uhlemann, E. G. Ström, and U. Bilstrup, "On the ability of the 802.11p mac method and stdma to support real-time vehicle-to-vehicle communication," *EURASIP J. Wirel. Commun. Netw.*, vol. 2009, pp. 5:1–5:13, Jan. 2009.

[31] ETSI TR 102 862, "Intelligent transport systems (ITS); on the recommended parameter setting for using STDMA for cooperative ITS; access layer part," December 2011.